7th International Building Physics Conference

IBPC2018

Proceedings

SYRACUSE, NY, USA

September 23 - 26, 2018

Healthy, Intelligent and Resilient Buildings and Urban Environments

ibpc2018.org | #ibpc2018

Numerical analysis of a ground-source heat-pump system in traditional Japanese "Kyo-machiya" dwellings

Shun Takano[1*], Chiemi Iba[1] and Shuichi Hokoi[2]

[1]Kyoto University, Japan
[2]Southeast University, China

[*]*Corresponding email: be.takanoshun@archi.kyoto-u.ac.jp*

ABSTRACT
Kyo-machiya, which is a traditional wooden dwelling in Kyoto, is generally equipped with a shallow well. The well water can be potentially utilized as a heat source with a geothermal heat-pump system without incurring a high drilling cost. Hereby, more energy saving in the traditional dwelling can be realized with the heat-pump system. However, an appropriate technique to utilize geothermal heat from a shallow well has not been established yet in Japan. To promote the geothermal use, we have continued an experiment to evaluate the practicability of a simple geothermal heat-pump system installed in a shallow well since the winter of 2013. In this study, the condition of the water flow in the well was examined using the computational fluid dynamics (CFD) technique, and the velocity of flow of the groundwater into the well was also estimated. We show that constant buoyancy was generated because of the temperature difference due to the heat-pump operation. Based on the results, a three-dimensional heat-transfer numerical analysis model, proposed in the previous study, was developed so that moisture transfer in the ground could be considered. Using the estimated buoyancy of the well water and the groundwater velocity, the calculated results seemed to reproduce the characteristic of the measured value. Furthermore, we show that the groundwater velocity has a large influence on the well water temperature.

KEYWORDS
Geothermal Heat Pump, Kyo-machiya, Well, Groundwater, CFD

INTRODUCTION
Geothermal heat is attractive as a stable energy source that is hardly affected by weather conditions and seasons. However, since the initial costs to utilize the geothermal heat such as those of drilling are very high, it is currently not widely used in Japanese dwellings (Nagano et al. 2006). Using geothermal heat, air conditioners can be operated without discharging cold air during winter. Additionally, the cooled ground can be used as a potentially cold heat source during summer. Since there are many unused shallow wells which were once used in a Kyo-machiya, a traditional wooden dwelling in Kyoto, energy saving may be realized by installing a ground-source heat pump (GSHP) system using the well water as the heat source, which will not involve a high initial cost. Therefore, the objective of this research is to spread the usage of GSHPs, which use the existing shallow wells in Japan, by providing basic information about the system and the efficient operational methods.
To promote the use of this system widely, it is necessary to evaluate the impact that this system has in real life and establish an optimum method whereby this system can be used. Hagihara et al. (2016) proposed a three-dimensional thermal model that can be used to predict the temperature change of the well water and showed the usefulness of the well water as a heat source. They also indicated that it is necessary for the well water to be restored to its original temperature for continuous heating. In their calculation, the water flow rate inside the well and

the inflow velocity of the groundwater into the well were estimated so that the calculation results agreed well with the measured results.
In this paper, we conducted a computational fluid dynamics (CFD) calculation to estimate the inflow velocity of the groundwater and the convective flow of the well water. Using the results, the heat and moisture transfer in and around the well during the heating operation was calculated by using the three-dimensional heat and moisture transfer model.

Nomenclatures			
c	Specific heat [J/kg·K]	ρ	Density [kg/m^3]
T	Temperature [K]	μ	Water chemical potential for free water [J/kg]
KS	Heat transfer coefficient [W/K]	λ	Thermal conductivity [W/(m·K)]
J	Flow rate [kg/m^2·s]	V	Volume [m^3]
A	Area [m^2]	n	Gravity coefficient [-]
r	Latent heat [J/kg]	$\partial/\partial n$	Normal direction differential on boundary between Well water and antifreeze solution pipe
g	Gravity acceleration [m/s^2]		
Subscripts			
w	Well water	s	Soil
a	Air	b	Antifreeze solution
g	Gas	c	Convection

Surveyed system and CFD Calculation

The surveyed heating system using well water is shown in Fig.1 (a). The measured well is about 9 m deep from the ground surface and about 80 cm in diameter (Fig.1 (b)). It is in the living room of a Kyo-machiya, Kyoto city. The GSHP system installed in this well has been operational since the winter of 2013. In this system, the heat-collecting pipe is in contact with the well water and antifreeze solution circulates in the pipe to exchange heat with well water. The well water temperature was measured at three different heights: 4500 mm (upper), 2500 mm (middle), and 500 mm (lower) from the bottom. Also, the depth of the well water, the heat-pump inlet/outlet temperatures of the antifreeze solution, and electricity consumption were measured.

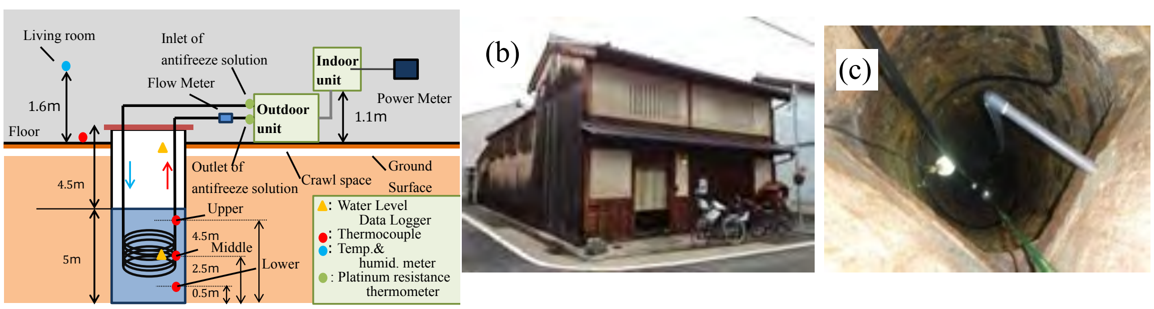

Fig.1 Surveyed system. (a) Schematics of measurement; (b) appearance of the Kyo-machiya; (c) well

Outline of the calculation

To simulate the characteristics of the temperature distribution of the well water when the heat pump was operated, and to clarify the water flow inside the well, a CFD analysis was performed. The simulation model is shown in Fig. 1(c) and (d), and the CFD calculation conditions are listed in Table 1. The model simulates the positional relation between the well and the antifreeze solution, and although the shapes of the well and the heat-collecting pipe are cylindrical, the shapes of these elements are approximated for simplicity as a square pipe of a volume and surface area equal to that of the actual well and the heat-collecting pipe, respectively. Based on the visual inspection of the well, the arrangement of the heat-collecting pipe was modelled to be concentrated at an approximate height of 3 m from the bottom. The CFD analysis software "Flow Designer 2017" was used for calculation.
According to a well drilling expert, the peripheral wall of this type of well is generally clogged

with mortar to the deep part and water does not easily permeate through it. Therefore, in this calculation, the groundwater was assumed to flow in only through the region which is 0.5 m from the bottom, which is different from that assumed in the previous study, (Hagihara et al. 2016) where the groundwater flows in through all parts of the well wall.

According to the literature (Fukukawa, 1969), several velocities of the groundwater were used to analyze the influence on the well water temperature by them. Only the results in case of a velocity of 2m/day, which agreed well with the measured results, were examined here. The remaining boundary surfaces were insulated.

The measured result during 07:30–13:00 h on December 22, 2015, which was the first day of the usage of heat pump during the winter, was used to verify the calculation.

(a)

(b)

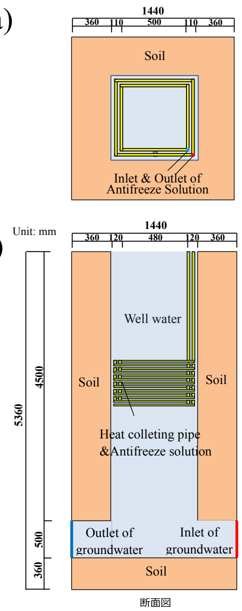

Table 1 Calculation condition

Space mesh number	X × Y × Z = 38 × 32 × 119 = 144,704
Size of calculated area	X × Y × Z = 1.44 × 1.44 × 5.36 m
Minimum mesh increment	15 mm
Time interval	0.1 s
Flow type	laminar flow
Temperature of groundwater	18.5 ℃
Velocity of groundwater	2.0 m/day
Inlet temperature of antifreeze solution	Given by the experimental result
Flowrate of antifreeze solution	

Fig.2(a) Computational domain of CFD (plan); (b) computational domain of CFD (vertical section) ; Table 1: Calculation condition

Results and discussion

Fig. 3 (a) shows the comparison between the calculated and the measured temperatures, and Figs. 3 (b) and (c) show the water flow during and after the heating operation, respectively.

The points of the antifreeze solution that were obtained from the measurement and calculation were different. The point obtained from the measurement was located in the living room, whereas the point obtained from the calculation was located in the well water because of the limited calculation domain. Therefore, both the temperatures may not be in agreement after the termination of the operation.

The calculated temperatures agree well with the measured results; thus, it can be said that the

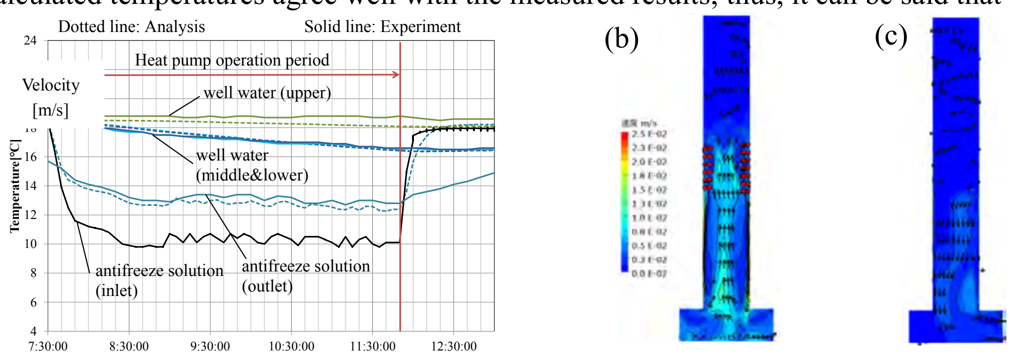

Fig. 3 Results of the CFD calculation. (a) Comparison of the calculated and measured temperatures. (b)(c) Water flow in the well: (b) 1 hour after the operation started and (c) 1 hour after the operation terminated.

inflow velocity of the groundwater and the location of the inflow inlet are accurately assumed. Fig. 3 (b) shows that water moves upward at about 0.01 m/s after commencing the heating operation. Since this upward flow did not occur after the heating was stopped, as shown in Fig. 3 (c), this water circulation was caused by the temperature difference between the inside and outside of the well. Judging from this result, the buoyant flow was taken into consideration in the three-dimensional heat and moisture analysis in the next section.

CALCULATION OF HEAT AND MOISTURE TRANSFER

Outline of calculation

A simulation model, as shown in Fig. 3, was proposed. The calculation area comprised soil, air, and water. The period considered for the calculation was from January 1, 2013 to January 16, 2014 (380 days), and the heating operation period was from December 27, 2013 to January 16, 2014 (20 days).

Therefore, on all sides of the calculation domain, the boundary temperature at a depth of more than 5 m was assumed to be 17.5°C, which was the annual average outdoor air temperature of Kyoto city (JMA 2014). The boundary temperature from the ground surface to a depth of 5 m was also approximated using the linear distribution by considering the results of one-dimensional thermal calculation. On the upper side of the calculation domain, three different values were used as the thermal boundary conditions: the temperature of the living room of the house (T_{room}); temperature of the crawl space (T_u); and temperature of the outside air (T_o). The inlet temperature (T_{in}) and the rate of flow of the antifreeze solution were also used as the boundary conditions.

The thermal conductance between the antifreeze solution and the well water as well as between the antifreeze solution and the well air are depicted in Fig. 3 as KS. Considering that the heat-collecting pipe was arranged in a bundle mainly in the middle height of the well, the thermal conductance was assumed to differ depending on the height.

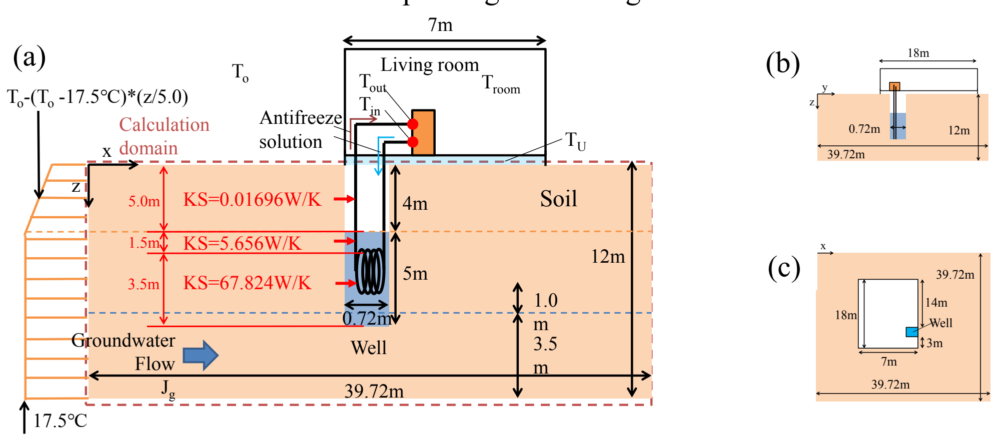

Fig. 4 Schematic of the simulation model: (a) x-z section; (b) y-z section; and (c) x-y plan

The equations (1)–(4) are the heat balance equations of the soil, well water, air in the well, and antifreeze solution proposed by Matsumoto et al. (1995); the basic equation of the groundwater flow is given by equation (5). The air in the well was dealt with as one mass. In the heat balance equation of the well water, both conductive and convective heat transfer were considered. From the results of the CFD analysis, it was assumed that the groundwater flow occurs by ground gradient, and the convective term by the groundwater flow is added to the heat balance equation. Table 2 shows the ground gradient coefficient and the liquid water conductivity related to the water chemical potential gradient. Also, from the results of the CFD analysis, it was assumed that a buoyant water flow of about 0.01 m/s occurs when the water temperature of the upper mesh is higher than that of the lower cell. In the calculation, two velocities of groundwater flow were considered; as assumed in the CFD analysis, one is 2 m/day, and the other is two times larger. The boundary conditions between the well water and well air, and the well water and the antifreeze solution are given by equations (6) and (7).

$$c_S\rho_S\frac{\partial T_S}{\partial t}=\nabla\left[\left(\lambda_S+r\lambda'_{s\ Tg}\right)\nabla T+r\lambda'_{s\ \mu g}\nabla\mu\right]-c_wJ_g\nabla T_S \tag{1}$$

$$c_w\rho_w\frac{\partial T_w}{\partial t}=\nabla(\lambda_w\nabla T_w)-c_wJ_{buo}\frac{\partial T_w}{\partial z}-c_wJ_c\frac{\partial T_w}{\partial x}-c_wJ_c\frac{\partial T_w}{\partial y} \tag{2}$$

$$c_a\rho_a\frac{\partial T_a}{\partial t}=-\sum\frac{K_aS_a}{V_a}(T_a-T_b)-\sum\alpha_iA_i(T_a-T_i) \tag{3}$$

$$c_b\rho_b\frac{\partial T_b}{\partial t}=\nabla(\lambda_b\nabla T_b)-c_bJ_{bx}\frac{\partial T_b}{\partial x}-c_bJ_{by}\frac{\partial T_b}{\partial y}-c_bJ_{bz}\frac{\partial T_b}{\partial z} \tag{4}$$

$$J_{gi}=-\lambda'_{i_\mu}\left(\frac{\partial\mu}{\partial i}-n_ig\right)\ (i=x,y,z) \tag{5}$$

$$-\lambda_w\frac{\partial T_w}{\partial z}=\alpha_a(T_a-T_w) \tag{6}$$

$$-\lambda_w\frac{\partial T_w}{\partial n}=K_w(T_b-T_w),-\lambda_b\frac{\partial T_b}{\partial n}=K_w(T_w-T_b) \tag{7}$$

Table 2 Moisture conductivity and ground gradient coefficient use in equation (5) (Z ≥ 8.5 m)

direction	n	λ'_μ [kg/ms(J/kg)]
x	0.017	1.5×10^{-4}–3.0×10^{-4}
y	0	0.0
z	0.999711	0.0

The material properties used are listed in Table 3. The density, specific heat, thermal conductivity, and moisture conductivity of the soil are assumed to change depending on its temperature and water content.

Table 3 Material properties used in the calculation

Material	c [J/kg·K]	λ [W/m·K]	ρ [kg/m^3]
Water	4,200	0.6	998
Air	1,005	(Heat transfer coefficient: 0.023[W/m^{2}K])	1.248
Antifreeze solution	4,100	0.5	1,020

Using these equations and conditions, the temperatures of the antifreeze solution and the well water were calculated. In the simulation, the space was discretized by using the central difference method and the time using forward difference. However, the heat balance equation of the antifreeze solution was discretized using the upwind difference method. The time increments were set as 0.15 s during the heating operation and 15 s in other cases.

Results and discussion

Figs. 5 (a) and 6 (b) compare the calculated temperatures of the well water with the measured results when the groundwater velocity was assumed to be 2 and 4 m/day, respectively. Figure 5 (c) compares the heat gain. In both cases (Figs. 5 (a) and 5 (b)), the measured tendency, i.e., that the water temperature in the upper region was higher than that in the middle and lower regions, was reproduced under the condition that the groundwater flows in only through the lower region of the well, which is different from that assumed in the previous study. Furthermore, it is likely that the groundwater velocity may be larger than that assumed in the CFD analysis since the result in (b) agrees with the measured result better than that from (a). Fig. 5 (c) shows that the heat gain is by 30% larger in the case of a groundwater velocity of 4 m/day. Thus, it can be said that the influence of the groundwater inflow on the well temperature

is very large.
However, shortly after beginning the calculation, the calculated well water temperature rapidly decreased as compared to the measured temperature, and the calculated upper temperature remained lower than the measured temperature. This may have occurred because the factors related to temperature recovery, such as infiltration of the ground water from the upper well wall, may not have been properly taken into consideration. To accurately evaluate the ground temperature and the water level of the well, it may be necessary to incorporate the aforementioned factors into the calculation model.

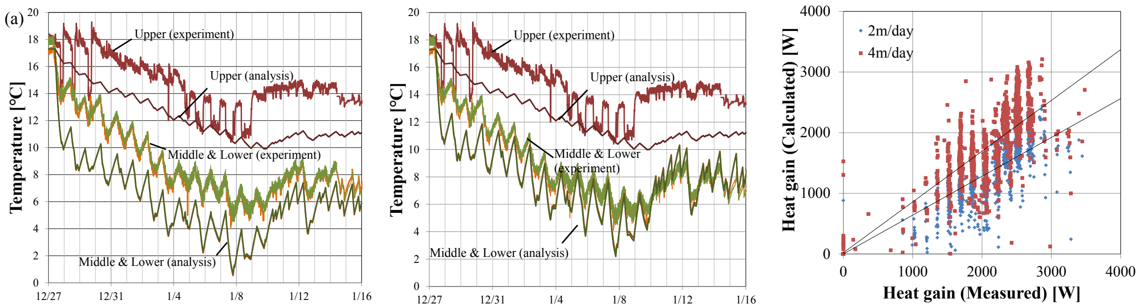

Fig. 5 Comparison of the calculated and measured results.
(a) Temperature (groundwater velocity of 2 m/day); (b) temperature (groundwater velocity of 4 m/day); (c) heat gain
(in Fig. 5(c), the measured heat gains are discretely distributed because they are calculated based on the measured temperatures in the units of 0.1℃)

CONCLUSION

In this study, the heat flow associated with water flow in and around the well with a heat-pump heating system was investigated by CFD analysis. It was shown that the water velocity due to the buoyancy amounted to about 0.01 m/s when the heating system was operated. Furthermore, previously proposed thermal model was extended to a heat and moisture transfer model based on the results of the CFD analysis, which show that the buoyancy and groundwater flow exist partially. The calculated results by the extended model agree well with the measured results that the water temperature in the upper region is higher than those in the middle and lower regions. It is also shown that the velocity of the groundwater has considerable impact on the well water temperature.

ACKNOWLEDGEMENT

The authors would like to thank the Kyo-machiya residents for their generous cooperation while setting up and using the heat pump.

REFERENCES

Advanced Knowledge Laboratory Inc.: Flow Designer 2017

Fukukawa Y, 1969, Functional deep well engineering, pp.4-13, Japan Road Technology Research Institute (in Japanese)

Hagihara K, Iba, C and Hokoi S, 2016, Effective use of a ground-source heat-pump system in traditional Japanese “Kyo-machiya” residences during winter, Energy and building, 128, pp.262-269

Japan Meteorological Agency 2014. URL: http://www.jma.go.jp/jma/index.html (Access date: 4 April 2018)

Matsumoto M, Nagai H, and Ushio T. Numerical analysis of thermal behavior in and around the thermal well: Experimental studies on application of the ground for annual heat storage part 2 [in Japanese], J. *of architecture, planning and environmental eng.* 1995, 470, pp.37-44

Nagano K, Katsura T, and Takeda S. , 2006, Development of a design and performance prediction tool for the ground source heat pump system, Applied Thermal Eng., 26, pp.1578-1592